

# La<sub>8+x</sub>Ti<sub>8+y</sub>S<sub>24</sub>O<sub>4</sub> Compounds Where $x + y \leq 2$ : A Series of Phases with Mixed-Valent Titanium

Louis J. Tranchitella, James C. Fettinger, Susan F. Heller-Zeisler, and Bryan W. Eichhorn\*

Center for Superconductivity Research and Department of Chemistry and Biochemistry, University of Maryland, College Park, Maryland 20742

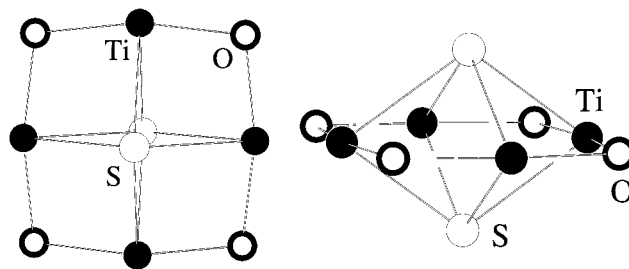
Received October 7, 1997. Revised Manuscript Received May 27, 1998

Three new titanium oxysulfides, La<sub>8.75</sub>Ti<sub>9.25</sub>S<sub>24</sub>O<sub>4</sub>, La<sub>8.50</sub>Ti<sub>9.50</sub>S<sub>24</sub>O<sub>4</sub>, and La<sub>8.10</sub>Ti<sub>8.05</sub>S<sub>24</sub>O<sub>4</sub>, were prepared by high-temperature methods (1025–1050 °C; ~80–150 h) from La<sub>2</sub>S<sub>3</sub>, Ti, S, and either La<sub>2</sub>O<sub>3</sub> or TiO<sub>2</sub> as oxygen sources. LaCl<sub>3</sub> (~10–30 wt %) was added as a flux. The compounds were characterized by single-crystal X-ray diffraction, neutron activation analysis, and EDX analysis. All three compounds contain common  ${}^2_{\infty}[(\text{Ti}_4\text{S}_2\text{O}_4)(\text{TiS}_6)_{4/2}]^{(12+\delta)-}$  oxysulfide layers and disordered/variable composition titanium sulfide layers that alternately stack along the *c*-axis of the unit cell. The titanium sulfide layers contain extensive La/Ti solid solution formation and are characterized by 5-fold disorders at the M(2) octahedral sites and 2-fold disorders at the M(3) sites. These compounds are members of a series of compounds with the general formula La<sub>8+x</sub>Ti<sub>8+y</sub>S<sub>24</sub>O<sub>4</sub>, where  $(x + y) \leq 2$  and the oxidation states of Ti can vary from +3 to +4. Crystal data (153 K) of La<sub>8.75</sub>Ti<sub>9.25</sub>S<sub>24</sub>O<sub>4</sub>: tetragonal space group *P4/mmm*, *a* = 10.4205(8) Å, *c* = 8.3848(6) Å, *V* = 910.5(1) Å<sup>3</sup>, *Z* = 1, *R*(*F*) = 3.88% and *wR*(*F*<sup>2</sup>) = 7.22%. For La<sub>8.50</sub>Ti<sub>9.50</sub>S<sub>24</sub>O<sub>4</sub>, tetragonal space group *P4/mmm*, *a* = 10.4101(3) Å, *c* = 8.396(1) Å, *V* = 909.9(1) Å<sup>3</sup>, *Z* = 1, *R*(*F*) = 3.54% and *wR*(*F*<sup>2</sup>) = 8.16%. For La<sub>8.10</sub>Ti<sub>8.05</sub>S<sub>24</sub>O<sub>4</sub>, tetragonal space group *P4/mmm*, *a* = 10.4212(3) Å, *c* = 8.233(2) Å, *V* = 894.1(2) Å<sup>3</sup>, *Z* = 1, *R*(*F*) = 4.25% and *wR*(*F*<sup>2</sup>) = 11.12%.

## Introduction

In the past few years, several oxysulfide phases of titanium have been reported by various research groups.<sup>1–5</sup> With one exception,<sup>1</sup> these compounds are structurally quite distinct from either the oxides or the sulfides of titanium and, in theory, allow one to blend the covalency of the sulfides with the ionicity of the oxides. It is apparent that the blending process causes structural complications. For example, many of the phases described to date suffer from disorder, complicated solid solution formation, and unusual coordination geometries.<sup>2,4</sup> Despite these differences, the compounds have a unique crystal chemistry and potentially novel properties.<sup>6–11</sup>

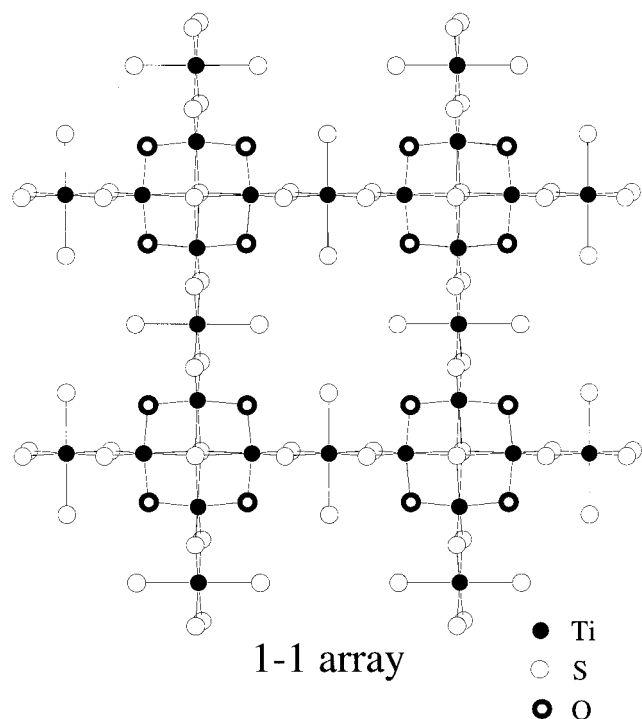
An interesting subset of these phases contains discrete [Ti<sub>4</sub>O<sub>4</sub>S<sub>2</sub>] cluster units which have now been identified in at least eight different compounds.<sup>3–5,12</sup> These clusters contain a square array of four Ti ions capped on top and bottom by a sulfide and are bridged along each Ti–Ti edge by oxide ions (see the drawing below). In many of the compounds, the clusters are



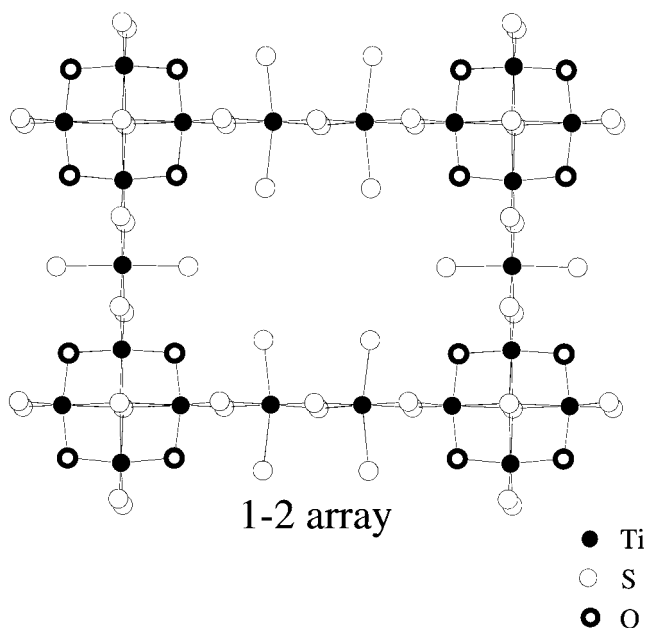
linked into two-dimensional arrays. In four of the compounds, the clusters are linked by single TiS<sub>6</sub> octahedra to form a 1–1 array in the *a*–*b* plane to form  ${}^2_{\infty}[(\text{Ti}_4\text{S}_2\text{O}_4)(\text{TiS}_6)_{4/2}]^{(12+\delta)-}$  layers (see the drawing below).<sup>4,12</sup> For the compound La<sub>20</sub>Ti<sub>11</sub>S<sub>44</sub>O<sub>6</sub>, the clusters are linked by a Ti<sub>2</sub>S<sub>10</sub> edge-shared bioctahedral dimer

- (1) Sutorik, A. C.; Kanatzidis, M. G. *Chem. Mater.* **1994**, *6*, 1700.
- (2) Cody, J. A.; Ibers, J. A. *J. Solid State Chem.* **1995**, *114*, 406.
- (3) Deudon, C.; Meerschaut, A.; Cario, L.; Rouxel, J. *J. Solid State Chem.* **1995**, *120*, 164.
- (4) Tranchitella, L. J.; Fettinger, J. C.; Eichhorn, B. W. *Chem. Mater.* **1996**, *8*, 2265.
- (5) Cody, J. A.; Deudon, C.; Cario, L.; Meerschaut, A. *Mater. Res. Bull.* **1997**, *32*, 1181.
- (6) Ouvrard, G.; Tchangbedji, G.; Deniard, P.; Prouzet, E. *Power Sources* **1995**, *54*, 246.
- (7) Schmidt, E.; Meunier, G.; Levasseur, A. *Solid State Ionics* **1995**, *76*, 243.
- (8) Levasseur, A.; Schmidt, E.; Meunier, G.; Gonbeau, D.; Benoist, L.; Pfisterguillouzo, G. *J. Power Sources* **1995**, *54*, 352.
- (9) Bizzak, D. J.; Chyu, M. K. *Rev. Sci. Instr.* **1994**, *65*, 102.
- (10) Bizzak, D. J.; Chyu, M. K. *Int. J. Heat Mass Trans.* **1995**, *38*, 1995.

- (11) Zhong, S. L.; Hepworth, M. T. *Energy Fuel* **1994**, *8*, 276.
- (12) Tranchitella, L. J.; Fettinger, J. C.; Eichhorn, B. W. To be published.



in one direction and a single  $\text{TiS}_6$  octahedron in the other to form a 1-2 array as shown below.<sup>3,5</sup> In both



cases, the clusters mark the intersections of orthogonal rutile-like chains that run through the lattice along the  $a$  and  $b$  axes. The oxidation states of Ti in these compounds can vary from +3 to +4 without significant changes in the oxysulfide layers. A wide variety of metal sulfides can be inserted between the oxysulfide cluster layers,<sup>4,12</sup> allowing one to electronically tune the oxidation state of Ti in these systems.

In a previous publication, we reported the synthesis and characterization of the first two phases containing 1-1 arrays.<sup>4</sup> These compounds,  $\text{Sr}_{5.8}\text{La}_{4.4}\text{Ti}_{7.8}\text{S}_{24}\text{O}_4$  and  $\text{La}_{14}\text{Ti}_8\text{S}_{33}\text{O}_4$ , contain identical  ${}^2_{\infty}[(\text{Ti}_4\text{S}_2\text{O}_4)(\text{TiS}_6)_{4/2}]^{12-}$  layers despite differences in composition and crystal symmetry. The oxidation state of titanium is +4 in

both. In that paper, we proposed that the tetragonal compound,  $\text{Sr}_{5.8}\text{La}_{4.4}\text{Ti}_{7.8}\text{S}_{24}\text{O}_4$ , may represent the end member of a solid solution in which Ti could be oxidized or reduced by adjusting the La:Sr:Ti ratios. This proposal was based on the small differences in refined compositions between the powders and single crystals of  $\text{Sr}_{5.8}\text{La}_{4.4}\text{Ti}_{7.8}\text{S}_{24}\text{O}_4$  and the fact that we had identified an all-lanthanum isomorphic end member with an approximate composition  $\text{La}_9\text{Ti}_9\text{S}_{24}\text{O}_4$ .<sup>4</sup> Subsequent analysis of this compound has shown its true composition to be  $\text{La}_{8.75}\text{Ti}_{9.25}\text{S}_{24}\text{O}_4$ . We report here the synthesis and structural details of  $\text{La}_{8.75}\text{Ti}_{9.25}\text{S}_{24}\text{O}_4$ , along with two closely related compounds of formula  $\text{La}_{8.50}\text{Ti}_{9.50}\text{S}_{24}\text{O}_4$  and  $\text{La}_{8.10}\text{Ti}_{8.05}\text{S}_{24}\text{O}_4$ . These three phases belong to the series of compounds defined by the general formula  $\text{La}_{8+x}\text{Ti}_{8+y}\text{S}_{24}\text{O}_4$ , where  $(x + y) \leq 2$ . Prior to the submission of this paper, we became aware that Cario et al. had prepared and structurally characterized another member of this series,  $\text{La}_8\text{Ti}_{10}\text{S}_{24}\text{O}_4$ , by a vastly different synthetic procedure.<sup>13</sup>

### Experimental Section

**Syntheses.**  $\text{LaCl}_3$  was recrystallized from HCl and dried under vacuum. All other reagents were purchased from CERAC and used without further purification. Single crystals of  $\text{La}_{8.75}\text{Ti}_{9.25}\text{S}_{24}\text{O}_4$  were prepared from  $\text{La}_2\text{S}_3$ , Ti,  $\text{TiO}_2$ , and S in a 1:1:1:1 ratio.  $\text{LaCl}_3$  was added as a flux (30 wt %). The starting materials were ground in an  $\text{N}_2$  drybox and loaded in a carbon-coated silica ampule. The ampule was sealed under vacuum and fired at 1025 °C for 78 h. The sample was cooled to 850 °C at 3 °C/h and then cooled to room temperature in 3 h. The sample was washed with ethanol and filtered to dissolve and remove the  $\text{LaCl}_3$  flux. The reaction yielded a black crystalline powder intermixed with small black single crystals (ca. 0.1 mm edges, ~5% of sample).

Single crystals of  $\text{La}_{8.50}\text{Ti}_{9.50}\text{S}_{24}\text{O}_4$  and  $\text{La}_{8.10}\text{Ti}_{8.05}\text{S}_{24}\text{O}_4$  were prepared from  $\text{La}_2\text{O}_3$ ,  $\text{La}_2\text{S}_3$ , Ti, and S in a 8:19:54:116 ratio.  $\text{LaCl}_3$  was added as a flux (10 and 20 wt % for  $\text{La}_{8.50}\text{Ti}_{9.50}\text{S}_{24}\text{O}_4$  and  $\text{La}_{8.10}\text{Ti}_{8.05}\text{S}_{24}\text{O}_4$ , respectively). The starting materials were ground in an  $\text{N}_2$  drybox and loaded in a carbon-coated silica ampule. The ampules were sealed under vacuum and fired at 1050 °C for 154 h for  $\text{La}_{8.50}\text{Ti}_{9.50}\text{S}_{24}\text{O}_4$  and at 1050 °C for 78 h for  $\text{La}_{8.10}\text{Ti}_{8.05}\text{S}_{24}\text{O}_4$ . The samples were cooled to 850 °C at 3 °C/h and then cooled to room temperature in 3 h. Each sample was washed with ethanol and filtered to dissolve and remove the  $\text{LaCl}_3$  flux. Both reactions yielded homogeneous black crystalline powders intermixed with small black single crystals ( $\text{La}_{8.50}\text{Ti}_{9.50}\text{S}_{24}\text{O}_4$ , ca. 0.1 mm edges, ~5% of sample;  $\text{La}_{8.10}\text{Ti}_{8.05}\text{S}_{24}\text{O}_4$ , ca. 0.15 mm edges, ~50% of sample).

Single crystals were analyzed by energy-dispersive X-ray analysis (EDX) on a JEOL JXA-840A electron probe microanalyzer. EDX on several crystals from each sample showed that La, Ti, and S were present in each single crystal. The EDX analyses of all the samples were complicated by the overlap of the La and Ti peaks which precluded semiquantitative analysis.

Crystals of  $\text{La}_{8.75}\text{Ti}_{9.25}\text{S}_{24}\text{O}_4$  and  $\text{La}_{8.10}\text{Ti}_{8.05}\text{S}_{24}\text{O}_4$  were analyzed by neutron activation analysis at the National Institute of Standards and Technology (NIST). Crystals with masses ranging from 1 to 3 mg, were weighed using a Model UMT2 microbalance and packaged in acid-cleaned polyethylene bags. Comparator standards were also prepared, using either elemental solutions pipetted onto small Whatman filter paper disks or solid primary standard compounds. Samples and standards were analyzed using instrumental neutron activation analysis (INAA), performed at the 20 MW research reactor at NIST. The principles of INAA have been previously

(13) Cario, L.; Deudon, C.; Meerschaut, A.; Rouxel, J. *J. Solid State Chem.* **1998**, *136*, 46.

**Table 1. Crystallographic Data for La<sub>8.75</sub>Ti<sub>9.25</sub>S<sub>24</sub>O<sub>4</sub>, La<sub>8.50</sub>Ti<sub>9.50</sub>S<sub>24</sub>O<sub>4</sub>, and La<sub>8.10</sub>Ti<sub>8.05</sub>S<sub>24</sub>O<sub>4</sub>**

	La <sub>8.75</sub> Ti <sub>9.25</sub> S <sub>24</sub> O <sub>4</sub> <sup>a</sup>	La <sub>8.50</sub> Ti <sub>9.50</sub> S <sub>24</sub> O <sub>4</sub>	La <sub>8.10</sub> Ti <sub>8.05</sub> S <sub>24</sub> O <sub>4</sub>
formula			
formula weight (amu)	2491.98	2469.23	2344.21
space group	<i>P4/mmm</i>	<i>P4/mmm</i>	<i>P4/mmm</i>
<i>a</i> (Å)	10.4205(8)	[10.4197(8)]	10.4101(3)
<i>b</i> (Å)	10.4205(8)	[10.4197(8)]	10.4101(3)
<i>c</i> (Å)	8.3848(6)	[8.382(1)]	8.396(1)
<i>V</i> (Å <sup>3</sup> )	910.48(12)	[910.0(3)]	909.9(1)
<i>T</i> (K)	153(2)		153(2)
<i>Z</i>	1		1
$\rho_{\text{cal}}$ (g/cm <sup>3</sup> )	4.545	[4.547]	4.506
no. of refln	1236	[1235]	963
no. of unique refln	663	[662]	520
no. unique refln with $F_o > 4\sigma F_o$	547	[570]	482
no. of variables <sup>b</sup>	52	[53]	55
radiation [Mo K $\alpha$ ] (Å)	0.71073		0.71073
$\mu$ (mm <sup>-1</sup> )	13.301	[13.308]	13.067
$R(F_o)^c$	3.88	[4.74]	3.54
$wR(F_o^2)^c$	7.22	[11.36]	8.16
GOF	1.088	[1.145]	1.200

<sup>a</sup> For La<sub>8.75</sub>Ti<sub>9.25</sub>S<sub>24</sub>O<sub>4</sub>, the numbers in brackets represent crystallographic data from a separate data set from a different crystal. Where no values are given, the data are the same from both refinements. <sup>b</sup> The number of variables differ for the reactions because some of the thermal parameters were refined isotropically or fixed in the final refinements of the data, as discussed in the crystallographic portion of the Experimental Section. <sup>c</sup>  $R(F_o) = [\sum(F_o - F_c)/\sum(F_o)]$  and  $wR(F_o^2) = [\sum w(F_o^2 - F_c^2)/\sum(F_o^2)]^{1/2}$ .

discussed.<sup>14</sup> The samples were irradiated at a neutron fluence rate of  $3.7 \times 10^{17}$  n m<sup>-2</sup> s<sup>-1</sup> for 2 min each. After suitable decay times, the samples and standards were measured on a 32% relative efficiency high-purity germanium  $\gamma$  spectrometer, with a resolution of 1.7 keV (FWHM at the 1332 photopeak of <sup>60</sup>Co with 6  $\mu$ s shaping time.). Measurement times were 5 min each. Data reduction, including computation of elemental concentrations, was accomplished using the Canberra/Nuclear Data activation analysis software package installed on a micro-VAX computer. The 320 keV line was utilized for quantitation of Ti-51, while multiple lines (328, 487, 815, and 1596 keV) were used for the quantitation of La-140. The results of the analysis are as follows (%): La<sub>8.75</sub>Ti<sub>9.25</sub>S<sub>24</sub>O<sub>4</sub>: calcd La 48.77, Ti 17.78; found La 48.6(3), Ti 15.5(2). For La<sub>8.10</sub>Ti<sub>8.05</sub>S<sub>24</sub>O<sub>4</sub>: calcd La 48.00, Ti 16.45; found La 48.8(1), Ti 14.9(1).

Powder X-ray diffraction data were collected at 25 °C on a Rigaku  $\theta$ - $\theta$  (Cu K $\alpha$ ) diffractometer in the  $10^\circ \leq 2\theta \leq 60^\circ$  range with a step width of 0.05°. The data were analyzed using an MDI software system. Bond valence analysis was performed using the methods and data of Brese and O'Keefe.<sup>15,16</sup>

**Structural Determinations.** La<sub>8.75</sub>Ti<sub>9.25</sub>S<sub>24</sub>O<sub>4</sub>. A shiny black cube with dimensions 0.10 × 0.10 × 0.09 mm was placed on the Enraf-Nonius CAD-4 diffractometer. The crystal's final cell parameters and crystal orientation matrix were determined from 25 reflections in the range  $19.8^\circ < 2\theta < 22.3^\circ$ . The cell constants were confirmed with axial photographs. Data were collected [Mo K $\alpha$ ] with  $\omega/2\theta$  scans over the range  $2.1^\circ < \theta < 27.5^\circ$  with a scan width of  $(0.90 + 0.52 \tan \theta)^\circ$  and a variable scan speed of 2.7–4.1 min<sup>-1</sup> with each scan recorded in 96 steps with the outermost 16 steps on each end of the scan being used for background measurement. Three nearly orthogonal standard reflections were monitored at 1 h intervals of X-ray exposure and showed negligible variations in intensity; data were not corrected. An absorption correction was applied on the basis of crystal faces with transmission factors ranging from 0.3136 to 0.3746. Data were corrected for Lorentz and polarization factors and reduced to  $F_o^2$  and  $\sigma(F_o^2)$  using the program XCAD4.<sup>17</sup> XPREP<sup>18</sup> was used to examine the data which, due to the lack of systematic absences along with intensity statistics, indicated the centrosymmetric space group *P4/mmm* (No. 123) as the most likely choice. XPREP<sup>18</sup> was also used to apply the absorption correction. The struc-

ture was determined by direct methods using the program XS.<sup>18</sup> Refinement with XL<sup>18</sup> and subsequent cycling and difference Fourier maps revealed the location of all of the atoms comprising the structure. Refinement of the structure converged well; however, it was apparent that several of the atoms were composites, being composed of partially occupied sites and solid solution of La and Ti. All atoms were refined anisotropically except Ti(2A), which had a fixed isotropic thermal parameter. The data were refined to convergence with  $[\Delta/\sigma \leq 0.001]$ ,  $R(F) = 3.88\%$ ,  $wR(F^2) = 7.22\%$  and GOF = 1.088 for all 663 unique reflections [ $R(F) = 2.81\%$ ,  $wR(F^2) = 6.80\%$  for those 547 data with  $F_o > 4\sigma(F_o)$ ]. A final difference Fourier map possessed large peaks within 1 Å of Ti(2A) and  $|\Delta\rho| \leq 3.7 \text{ e } \text{Å}^{-3}$ . A second data set for this compound was collected from an independent crystal. The results of the refinement were the same (see Table 1 and the Results section).<sup>19</sup>

La<sub>8.50</sub>Ti<sub>9.50</sub>S<sub>24</sub>O<sub>4</sub>. A shiny black hexagonal block with dimensions 0.15 × 0.125 × 0.10 mm was placed on the Enraf-Nonius CAD-4 diffractometer. Data were collected and processed as described above. Six standard reflections were monitored at 30 min intervals of X-ray exposure and showed negligible variations in intensity; data were not corrected. Five  $\Psi$  scan reflections were collected over the range  $5.9^\circ < \theta < 18.6^\circ$ ; the absorption correction was applied with transmission factors ranging from 0.0817 to 0.1495. All atoms were refined anisotropically except Ti(2A), which was refined isotropically, and the data were refined to convergence with  $[\Delta/\sigma \leq 0.001]$ ,  $R(F) = 3.54\%$ ,  $wR(F^2) = 8.16\%$  and GOF = 1.200 for all 520 unique reflections [ $R(F) = 3.28\%$ ,  $wR(F^2) = 8.01\%$  for those 482 data with  $F_o > 4\sigma(F_o)$ ]. A final difference Fourier map possessed large peaks within 1 Å of Ti(2A) and  $|\Delta\rho| \leq 2.5 \text{ e } \text{Å}^{-3}$ .

La<sub>8.10</sub>Ti<sub>8.05</sub>S<sub>24</sub>O<sub>4</sub>. A shiny silver hexagonal shaped cylinder with dimensions 0.425 × 0.250 × 0.150 mm was placed on the Enraf-Nonius CAD-4 diffractometer. Data were collected and processed as described above. Six standard reflections were monitored at 30 min intervals of X-ray exposure and showed negligible variations in intensity; data were not corrected. Six  $\Psi$  scan reflections were collected over the range  $5.9^\circ < \theta < 19.0^\circ$ ; the absorption correction was applied with transmission factors ranging from 0.0137 to 0.0634. All atoms were refined anisotropically except La(2), Ti(2A), and Ti(3), and the data were refined to convergence with  $[\Delta/\sigma \leq 0.001]$ ,  $R(F) = 4.25\%$ ,  $wR(F^2) = 11.12\%$ , and GOF = 1.182 for all 512 unique reflections [ $R(F) = 4.08\%$ ,  $wR(F^2) = 10.97\%$  for those 491 data with  $F_o > 4\sigma(F_o)$ ]. A final difference Fourier map possessed large peaks within 1 Å of Ti(2A) and  $|\Delta\rho| \leq 2.6 \text{ e } \text{Å}^{-3}$ .

(14) Greenberg, R. R.; Fleming, R. F.; Zeisler, R. *Environ. Intern.* **1984**, *10*, 129.

(15) O'Keefe, M. *Acta Crystallogr. A* **1990**, *46*, 138.

(16) Brese, N. E.; O'Keefe, M. *Acta Crystallogr. B* **1991**, *47*, 192.

(17) Harms, K. *XCAD4*. Program for the Lp-correction of Nonius CAD-4 diffractometer data; University of Marburg, Germany, 1993.

(18) Sheldrick, G. M. *SHELXTL*. Version 5.03.; Siemens Analytical X-ray Instruments Inc.: Madison, WI, 1994.

(19) The *c*-axis of the two refinements differed by 2 $\sigma$ .



All three compounds exhibit disorder at the M(2) site, with lanthanum [La(2)] present at the center of a  $S_6$  octahedron and titanium [Ti(2A)] present on a 4-fold disorder site around the lanthanum atom. Initially, the models contained only lanthanum at the M(2) site and then with a mixture of lanthanum and titanium. The summed occupancies were constrained to be 100% (i.e. only one metal atom was present at any given time) and the isotropic thermal parameters were linked using an EADP<sup>18</sup> instruction. The electron density difference maps exhibited large peaks that generated a 4-fold disorder less than 1 Å from M(2). In an attempt to model this electron density, lanthanum and titanium were placed at the central M(2) site and titanium was placed at the 4-fold disordered Ti(2A) site. The total occupancy for the site, M(2) + Ti(2A), was once again constrained using a SUMP<sup>18</sup> instruction to be 100% and the isotropic thermal parameters were linked using an EADP<sup>18</sup> instruction. Refinement of this model against the three different data sets gave 0% titanium occupancy on the central M(2) site of each compound. The three compounds differed in the *relative* occupancy of the central La(2) site and Ti(2A) sites, but the elements remained completely segregated in each. Once the occupancies no longer varied, they were fixed at the refined values, the EADP<sup>18</sup> instructions were removed, and the models were refined with all atoms being anisotropic. In a few instances, some atoms became nonpositive definite and had to be refined isotropically or fixed at the linked isotropic value reported (as noted above). In each case, the electron density difference maps exhibited a peak Q(1) at 0.0000, ~0.08, 0.5, within ~0.5 Å of Ti(2A). This site exhibits a 4-fold disorder around La(2) similar to Ti(2A) but is rotated by 45° in the *a*-*b* plane. Attempts to model this peak as a partially occupied titanium atom resulted in an occupancy of 0. It was concluded that these large peaks ~2.5–3.7 e Å<sup>-3</sup> in all three compounds were due to termination errors.

The M(3) sites contain a solid solution of lanthanum and titanium statistically disordered over two positions. The two sites lie approximately 1 Å from each other across a mirror plane. Initially, the models were constructed with titanium at the M(3) site with an occupancy of 50% (i.e. only one atom was present at any given time). The thermal parameters were extremely small, sometimes negative, suggesting that lanthanum was present along with titanium. After linking the isotropic thermal parameters of La(3) and Ti(3) using an EADP instruction and constraining the total occupancy of the M(3) site to be 50%, the relative occupancies of La and Ti were refined. Once the occupancies of La and Ti no longer varied, the occupancy of each atom was fixed at the refined value and the atoms were refined anisotropically.

A much smaller peak appeared in the electron density difference map at the M(3) position of La<sub>8.10</sub>Ti<sub>8.05</sub>S<sub>24</sub>O<sub>4</sub> relative to the other compounds. It exhibited the same type of behavior as that previously mentioned, with metal atoms disordered over two positions that lie approximately 1 Å from each other across a mirror plane. Initially the data were refined with titanium at the M(3) site with an occupancy of 50%. However, the thermal parameters were extremely large, suggesting that the site was only partially occupied. This hypothesis was confirmed by refining the occupancy which gave a 6.4% population. Once the occupancy no longer varied, it was fixed and the data were refined with Ti(3) isotropic.

## Results

**A. Synthesis and Characterization.** The compounds La<sub>8.75</sub>Ti<sub>9.25</sub>S<sub>24</sub>O<sub>4</sub> (**I**), La<sub>8.50</sub>Ti<sub>9.50</sub>S<sub>24</sub>O<sub>4</sub> (**II**), and La<sub>8.10</sub>Ti<sub>8.05</sub>S<sub>24</sub>O<sub>4</sub> (**III**) were prepared from the elements and binaries at 1025–1050 °C. Oxygen was introduced into the reactions by using TiO<sub>2</sub> or La<sub>2</sub>O<sub>3</sub>, and single crystals were only obtained with the use of LaCl<sub>3</sub> fluxes. The compounds were characterized by single-crystal X-ray diffraction, powder X-ray diffraction (XRD), energy-dispersive X-ray analysis (EDX), and neutron activation

analysis (for **I** and **III**). Analysis of the XRD profiles for the bulk reaction mixtures of **II** and **III** indicated the “oxysulfide” was the major phase, with minor unidentifiable phases present. Because the XRD profiles for all of the tetragonal La<sub>8+x</sub>Ti<sub>8+y</sub>S<sub>24</sub>O<sub>4</sub> phases are virtually identical, the compositions of the bulk powders were not discernible. The XRD profile for the bulk reaction mixture of **I** exhibited TiS<sub>2</sub> as the major phase, with only trace amounts of **I**. Exhaustive efforts to prepare single-phase bulk samples by using stoichiometric ratios of reagents and changing reaction times, temperatures, and flux charges were unsuccessful. The EDX studies on crystals from each set of reactions showed that all the constituent elements were present, but quantitative analysis was hindered by the overlap of La and Ti peaks. Neutron activation studies (optimized for La analysis) on single-crystal samples of **I** and **III** showed good agreement between the observed La content and the crystallographically refined La contents from the single-crystal analysis (see below). The Ti content in both samples was lower than expected in the neutron activation studies. The source of the difference is unclear at present, but further studies are in progress.

**B. Solid State Structures. General.** All three compounds are tetragonal, space group *P4/mmm*, and are quite similar in structure to Sr<sub>5.8</sub>La<sub>4.4</sub>Ti<sub>7.8</sub>S<sub>24</sub>O<sub>4</sub>.<sup>4</sup> Summaries of the crystallographic data for **I–III** are given in Table 1. Atomic coordinates, equivalent isotropic displacement parameters and fractional occupancies for **I–III** are given in Table 2. Selected interatomic distances and bond angles are listed in Table 3.

The presence of two disordered La<sub>1-x</sub>Ti<sub>x</sub> atomic sites in all three compounds complicated the structural refinements. Therefore, several structural models were analyzed in each crystallographic refinement. The final model chosen for each compound was selected on the basis of the chemical requirements (i.e. charge and size) and successful crystallographic refinements. The refinement of a second independent data set from a different crystal of La<sub>8.75</sub>Ti<sub>9.25</sub>S<sub>24</sub>O<sub>4</sub> gave the same solution in that the final composition, unit cell, and bond distances and angles were identical within one standard deviation.<sup>19</sup> However, there are significant differences among **I–III** in terms of unit cells, compositions, occupancies, and metric parameters.

The general structure of the La<sub>8+x</sub>Ti<sub>8+y</sub>S<sub>24</sub>O<sub>4</sub> compounds can be viewed as  ${}^2_{\infty}[(Ti_4S_2O_4)(TiS_6)_{4/2}]^{(12+\delta)-}$  oxysulfide layers and variable composition, disordered titanium sulfide layers that alternately stack along the *c*-axis of the unit cell (see Figure 1). The two layers share several common edges and vertices, giving rise to a highly connected three-dimensional structure. A nine-coordinate La<sup>3+</sup> ion resides in the tricapped trigonal prismatic “OS<sub>8</sub>” holes formed at the interstices of the two layers. The  ${}^2_{\infty}[(Ti_4S_2O_4)(TiS_6)_{4/2}]^{(12+\delta)-}$  oxysulfide sheet is essentially the same in each compound, showing only slight variations in bond distances and angles. In contrast, the layer separating the oxysulfide sheets is highly adaptive in terms of composition and crystallographic disorder and is significantly different in **I–III**. The two layers are described separately below.

*The Common  ${}^2_{\infty}[(Ti_4S_2O_4)(TiS_6)_{4/2}]^{(12+\delta)-}$  Layers.* The  ${}^2_{\infty}[(Ti_4S_2O_4)(TiS_6)_{4/2}]^{(12+\delta)-}$  oxysulfide layer of **I** as viewed down the *c*-axis is given in Figure 2a. This layer

**Table 2. Atomic Coordinates, Equivalent Isotropic Displacement Parameters ( $\text{\AA}^2$ ),<sup>a</sup> and Site Occupancy Factors<sup>b</sup> for  $\text{La}_{8.75}\text{Ti}_{9.25}\text{S}_{24}\text{O}_4$  (I),  $\text{La}_{8.50}\text{Ti}_{9.50}\text{S}_{24}\text{O}_4$  (II), and  $\text{La}_{8.10}\text{Ti}_{8.05}\text{S}_{24}\text{O}_4$  (III)**

atom	parameter	I	II	III
La(1)	<i>x</i>	0.2916(1)	0.2911(1)	0.2924(1)
	<i>y</i>	0.2916(1)	0.2911(1)	0.2924(1)
	<i>z</i>	0.2371(1)	0.2369(1)	0.2417(1)
	<i>U</i> (eq)	0.010(1)	0.014(1)	0.014(1)
	occ	0.192	0.244	0.108
La(2)	<i>x</i>	0	0	0
	<i>y</i>	0	0	0
	<i>z</i>	0.5000	0.5000	0.5000
	<i>U</i> (eq)	0.012(2)	0.015(2)	0.005(3) <sup>c</sup>
	occ	0.192	0.244	0.108
Ti(2A)	<i>x</i>	0.0560(9)	0.0531(10)	0.0557(7)
	<i>y</i>	0.0560(9)	0.0531(10)	0.0557(7)
	<i>z</i>	0.5000	0.5000	0.5000
	<i>U</i> (eq)	0.006 <sup>c</sup>	0.011(3) <sup>c</sup>	0.0(2) <sup>c</sup>
	occ	0.808	0.756	0.892
La(3)	<i>x</i>	0	0	0
	<i>y</i>	0.4531(4)	0.4496(4)	0.4496(4)
	<i>z</i>	0.5000	0.5000	0.5000
	<i>U</i> (eq)	0.015(1)	0.011(1)	0.011(1)
	occ	0.140	0.062	0.062
Ti(3)	<i>x</i>	0	0	0
	<i>y</i>	0.4531(4)	0.4496(4)	0.4392(78)
	<i>z</i>	0.5000	0.5000	0.5000
	<i>U</i> (eq)	0.015(1)	0.011(1)	0.009(14) <sup>c</sup>
	occ	0.360	0.438	0.064
Ti(1)	<i>x</i>	0	0	0
	<i>y</i>	0.5000	0.5000	0.5000
	<i>z</i>	0	0	0
	<i>U</i> (eq)	0.008(1)	0.012(1)	0.015(1)
Ti(4)	<i>x</i>	0.5000	0.5000	0.5000
	<i>y</i>	0.5000	0.5000	0.5000
	<i>z</i>	0.5000	0.5000	0.5000
	<i>U</i> (eq)	0.019(1)	0.028(1)	0.019(1)
Ti(5)	<i>x</i>	0	0	0
	<i>y</i>	0.2046(2)	0.2054(2)	0.2066(2)
	<i>z</i>	0	0	0
	<i>U</i> (eq)	0.009(1)	0.014(1)	0.013(1)
S(1)	<i>x</i>	0.5000	0.5000	0.5000
	<i>y</i>	0.5000	0.5000	0.5000
	<i>z</i>	0.2231(6)	0.2245(6)	0.2183(6)
	<i>U</i> (eq)	0.007(1)	0.011(1)	0.013(1)
S(2)	<i>x</i>	0.2347(3)	0.2352(3)	0.2343(4)
	<i>y</i>	0.5000	0.5000	0.5000
	<i>z</i>	0	0	0
	<i>U</i> (eq)	0.006(1)	0.011(1)	0.014(1)
S(3)	<i>x</i>	0	0	0
	<i>y</i>	0.3428(2)	0.3431(2)	0.3430(3)
	<i>z</i>	0.2204(3)	0.2201(3)	0.2206(3)
	<i>U</i> (eq)	0.011(1)	0.016(1)	0.014(1)
S(4)	<i>x</i>	0.7402(3)	0.7391(3)	0.7393(4)
	<i>y</i>	0.5000	0.5000	0.5000
	<i>z</i>	0.5000	0.5000	0.5000
	<i>U</i> (eq)	0.010(1)	0.014(1)	0.015(1)
S(5)	<i>x</i>	0	0	0
	<i>y</i>	0	0	0
	<i>z</i>	0.1793(6)	0.1807(7)	0.1821(6)
	<i>U</i> (eq)	0.009(1)	0.014(1)	0.015(1)
S(6)	<i>x</i>	0.1702(4)	0.1690(4)	0.1643(3)
	<i>y</i>	0.1702(4)	0.1690(4)	0.1643(3)
	<i>z</i>	0.5000	0.5000	0.5000
	<i>U</i> (eq)	0.033(1)	0.037(1)	0.026(1)
O(1)	<i>x</i>	0.1873(6)	0.1872(7)	0.1846(8)
	<i>y</i>	0.1873(6)	0.1872(7)	0.1846(8)
	<i>z</i>	0	0	0
	<i>U</i> (eq)	0.008(2)	0.014(2)	0.015(2)

<sup>a</sup> *U*(eq) is defined as one-third of the trace of the orthogonalized  $U_{ij}$  tensor. <sup>b</sup> Sites are fully occupied unless noted in table. <sup>c</sup> Refined isotropically.

**Table 3. Selected Interatomic Distances ( $\text{\AA}$ ) and Angles (deg) for  $\text{La}_{8.75}\text{Ti}_{9.25}\text{S}_{24}\text{O}_4$  (I),  $\text{La}_{8.50}\text{Ti}_{9.50}\text{S}_{24}\text{O}_4$  (II), and  $\text{La}_{8.10}\text{Ti}_{8.05}\text{S}_{24}\text{O}_4$  (III)**

bond	mult	I <sup>a</sup>	II	III
La(1)–O(1)		2.513(6)	[2.507(6)]	2.509(6)
La(1)–S(6)		2.840(3)	[2.843(3)]	2.848(3)
La(1)–S(2)	2×	3.003(1)	[3.002(1)]	3.004(1)
La(1)–S(1)		3.074(1)	[3.074(1)]	3.077(1)
La(1)–S(3)	2×	3.088(1)	[3.088(1)]	3.082(1)
La(1)–S(4)	2×	3.113(1)	[3.113(1)]	3.116(1)
La(2)–Ti(2A)	4×	0.826(14)	[0.850(12)]	0.78(2)
La(2)–S(6)	4×	2.507(5)	[2.503(5)]	2.488(5)
La(2)–S(5)	2×	2.690(5)	[2.686(5)]	2.681(5)
Ti(2A)–Ti(2A)	2×	1.168(20)	[1.203(17)]	1.10(2)
Ti(2A)–Ti(2A)		1.651(28)	[1.653(13)]	1.56(3)
Ti(2A)–S(6)		1.684(15)	[1.701(24)]	1.726(16)
Ti(2A)–S(6)	2×	2.640(7)	[2.644(6)]	2.608(7)
Ti(2A)–S(5)	2×	2.813(7)	[2.817(6)]	2.792(7)
Ti(2A)–S(6)		3.333(15)	[3.354(13)]	3.27(2)
M(3)–M(3)		0.978(8)	[0.977(8)]	1.049(8)
M(3)–S(3)	2×	2.611(3)	[2.613(3)]	2.598(3)
M(3)–S(4)	2×	2.751(4)	[2.755(4)]	2.767(4)
M(3)–S(3)	2×	3.165(4)	[3.167(4)]	3.190(4)
Ti(1)–S(2)	2×	2.446(3)	[2.448(3)]	2.448(3)
Ti(1)–S(3)	4×	2.469(2)	[2.470(2)]	2.466(2)
Ti(1)–Ti(5)	2×	3.079(3)	[3.078(2)]	3.067(2)
Ti(4)–S(1)	2×	2.332(5)	[2.316(5)]	2.313(5)
Ti(4)–S(4)	4×	2.503(4)	[2.499(3)]	2.489(4)
Ti(5)–O(1)	2×	1.960(6)	[1.965(6)]	1.958(6)
Ti(5)–S(3)	2×	2.343(3)	[2.341(3)]	2.339(3)
Ti(5)–S(5)	2×	2.608(4)	[2.611(4)]	2.622(4)
Ti(5)–Ti(5)	2×	3.015(4)	[3.016(3)]	3.024(3)
angle		I	II	III
O(1)–Ti(5)–O(1)		169.5(4)	[169.8(5)]	168.9(5)
S(3)–Ti(5)–S(3)		104.1(2)	[104.2(2)]	104.4(2)
O(1)–Ti(5)–S(5)		85.7(2)	[85.8(2)]	85.5(2)
S(5)–Ti(5)–S(5)		70.4(2)	[70.5(2)]	70.7(2)
Ti(5)–O(1)–Ti(5)		100.5(4)	[100.2(5)]	101.1(5)

<sup>a</sup> For  $\text{La}_{8.75}\text{Ti}_{9.25}\text{S}_{24}\text{O}_4$  (I) the numbers in brackets represent crystallographic data from a separate refinement on a different crystal.

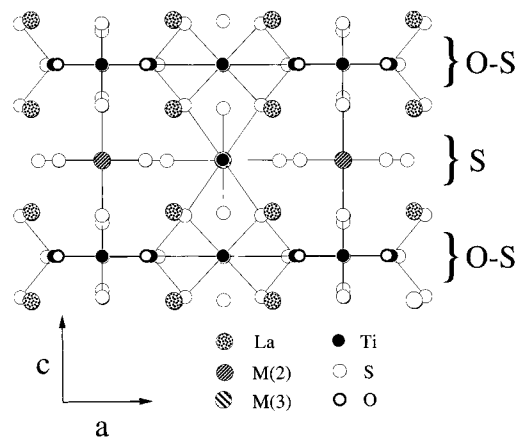


**Figure 1.** Approximate (100) projection of  $\text{La}_{8.75}\text{Ti}_{9.25}\text{S}_{24}\text{O}_4$  showing the alternating layers along the *c*-axis. The bold lines represent the unit cell, O–S denotes the oxysulfide  ${}_{\infty}[(\text{Ti}_4\text{S}_2\text{O}_4)(\text{TiS}_{6/4/2})^{(12+\delta)-}]$  layer, and S denotes the sulfide-only layer.

contains  $\text{Ti}_4\text{S}_2\text{O}_4$  clusters arranged such that the capping  $\mu_4\text{-S}(5)$  atoms reside on the *c*-axis of the unit cell (the 4-fold rotation axis). The clusters are linked in the *a*–*b* plane by sharing edges with the Ti(1) $\text{S}_6$  octahedra to form an infinite square net of formula  ${}_{\infty}[(\text{Ti}_4\text{S}_2\text{O}_4)(\text{TiS}_{6/4/2})^{(12+\delta)-}]$ . The Ti(1)–S distances are quite regular with average contacts of 2.46(1)  $\text{\AA}$  in all three compounds. The Ti(5) atoms in the  $\text{Ti}_4\text{S}_2\text{O}_4$  cluster are

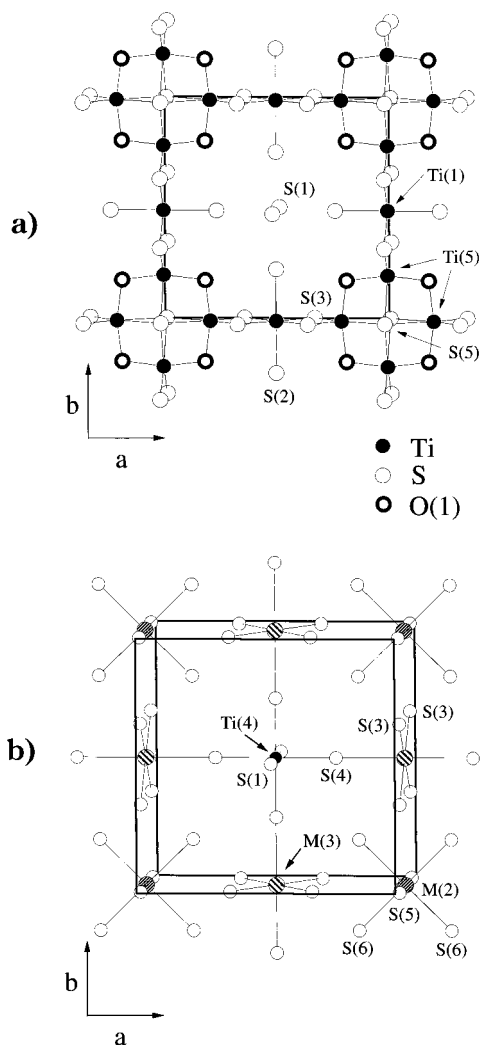


**Figure 2.** (a) A (001) projection of the  ${}^2_{\infty}[(\text{Ti}_4\text{S}_2\text{O}_4)(\text{TiS}_6)_{4/2}]^{(12+\delta)-}$  layer (the O–S layer) in **I**. (b) (001) projection showing the general positional arrangement of the sites in the disordered sulfide layer (the S layer) of the  $\text{La}_{8+x}\text{Ti}_{9-x}\text{S}_{24}\text{O}_4$  series. The bold lines represent the unit cell.

in distorted  $\text{TiO}_2\text{S}_4$  octahedral environments. The Ti(5)–S(5) distances are 2.608(4), 2.622(4), and 2.624(4) Å, the Ti(5)–S(3) distances are 2.343(3), 2.339(3), and 2.307(3) Å, and the Ti(5)–O(1) distances are 1.960(6), 1.958(6), and 1.937(7) Å for **I**, **II** and **III**, respectively. The Ti–O distances are in good agreement with the reported Ti–O distances of  $\sim 1.95$ – $1.97$  Å in  $\text{TiO}_2$ .<sup>20</sup> The Ti–S contacts are close to the reported values for octahedral Ti–S distances in related compounds ( $d_{\text{Ti-S}} \sim 2.4$  Å ave).<sup>21</sup> An empty  $\text{S}_6$  octahedron resides in the center of the square nets and are defined by four S(2) atoms and two S(1) atoms from neighboring layers.

*The Disordered/Variable Composition Sulfide Layer.* Separating each  ${}^2_{\infty}[(\text{Ti}_4\text{S}_2\text{O}_4)(\text{TiS}_6)_{4/2}]^{(12+\delta)-}$  oxysulfide layer is a disordered layer containing three distinct polyhedral sites: a Ti(4) $\text{S}_6$  octahedron, one M(2) $\text{S}_6$  octahedron, and two M(3) $\text{S}_6$  octahedra (see Figure 2b), where M is a combination of La and Ti. The central Ti(4) $\text{S}_6$  octahedron shares its four corners in the  $a$ – $b$

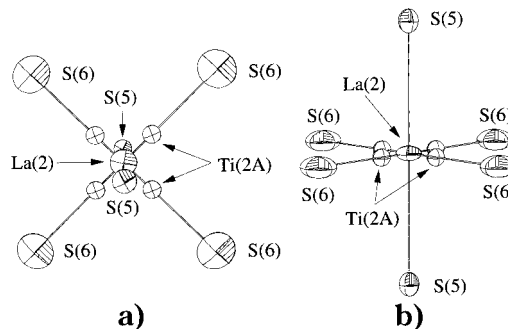


**Figure 3.** (a) ORTEP drawing of an approximate (001) projection of the M(2) site in  $\text{La}_{8.75}\text{Ti}_{9.25}\text{S}_{24}\text{O}_4$ . (b) ORTEP drawing of an approximate (100) projection of the M(2) site for  $\text{La}_{8.75}\text{Ti}_{9.25}\text{S}_{24}\text{O}_4$ .

plane with four M(3) $\text{S}_6$  octahedra forming a two-dimensional square net. Each neighboring octahedron is rotated by  $45^\circ$  about the Ti(4)–S(4)–M(3) vectors. The M(3) $\text{S}_6$  octahedra share common edges with the Ti(1)– $\text{S}_6$  octahedra in the  ${}^2_{\infty}[(\text{Ti}_4\text{S}_2\text{O}_4)(\text{TiS}_6)_{4/2}]^{(12+\delta)-}$  layers to form rutile-like edge-sharing chains that run parallel to the  $c$ -axis. The M(2) $\text{S}_6$  octahedra fill the holes in the square net and link the  $\text{Ti}_4\text{S}_2\text{O}_4$  clusters from adjacent oxysulfide layers along the  $c$ -axis.

The Ti(4)–S(4) distances are 2.503(4), 2.489(4), and 2.493(4) Å in **I**–**III**, respectively. The respective Ti(4)–S(1) distances are shorter at 2.322(5), 2.313(5), and 2.319(5) Å. The shorter contacts to S(1) relative to S(4) are expected since S(1) is essentially one-coordinate (in terms of Ti–S bonds), bound to only Ti(4), and is the apical sulfur atom of the empty  $\text{S}_6$  octahedron formed by the intersecting rutile-like chains in the oxysulfide layer.

The M(2) “site” is disordered over five positions and contains variable amounts of La and Ti in the three compounds. The  $\text{La}_{1-x}\text{Ti}_x\text{S}_6$  octahedron (see Figure 3), contains four S(6) atoms in the  $a$ – $b$  plane and two S(5) atoms along the  $c$ -axis. The lanthanum atom La(2) resides at the center of the octahedron and the titanium Ti(2A) atoms are disordered about a 4-fold rotation axis, approximately 0.8 Å from the lanthanum along the La–S(6) vectors. The amounts of lanthanum and titanium on the M(2) sites were refined such that the total occupancy of the octahedron was 100%. The refined ratios of La:Ti are 0.192:0.808 in **I**, 0.244:0.756 in **II**, and 0.108:0.892 in **III**. Due to the five different metal atom positions at the M(2) site, the S(6) positions represent an average or “composite” of the five different polyhedra present (four  $\text{TiS}_5$  square pyramids and one  $\text{LaS}_6$  octahedron, see below). This composite character is evidenced by the disk-like shape of the S(6) thermal ellipsoids (Figure 3). As a result, the S(6) position is an average of five different positions; thus, distances to S(6) are not meaningful in terms of finding accurate M–S separations. However, the general trends in distances are consistent with expectations based on the site occupancies and distances to S(5).

Due to the larger size of  $\text{La}^{3+}$  relative to  $\text{Ti}^{3+/4+}$  (VI coordinate  $\text{La}^{3+}$ ,  $r_i = 1.03$  Å; VI coordinate  $\text{Ti}^{3+}$ ,  $r_i = 0.67$  Å; VI coordinate  $\text{Ti}^{4+}$ ,  $r_i = 0.605$  Å),<sup>22</sup> the average M(2) octahedral hole increases in size as the  $\text{La}^{3+}$

(20) West, A. R. *Basic Solid State Chemistry*; John Wiley & Sons: New York, 1991.

(21) Eichhorn, B. W. *Prog. Inorg. Chem.* **1994**, *42*, 139.

(22) Shannon, R. D. *Acta Crystallogr.* **1976**, *A32*, 751.



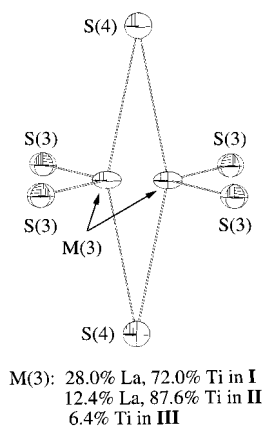


**Figure 4.** ORTEP drawing of the M(3) site in  $\text{La}_{8.75}\text{Ti}_{9.25}\text{S}_{24}\text{O}_4$ .

occupancy increases at the M(2) site. Statistically, it is difficult to discern differences between the overall "size" of the  $\text{S}_6$  octahedral hole in **I** and **II** based on the average La–S distances; however, in **III**, the  $\text{La}(2)\text{S}_6$  octahedron is clearly the smallest out of the three. For example, the La(2)–S(5) distances are 2.689(5), 2.681(5), and 2.617(5) Å in **I**, **II** and **III**, respectively, and the La(2)–S(6) composite distances show a similar trend.

Although La(2) appears to be in a fairly regular octahedral site, Ti(2A) is significantly off-center in the octahedral cavity in a distorted square pyramidal environment. For **I–III**, the apical Ti(2A)–S(6) bonds appear to be anomalously short at  $\sim 1.65$  Å, but since S(6) is a composite site, the actual distance is surely much longer. The base of the square pyramid is defined by two longer Ti(2A)–S(6) interactions ranging  $\sim 2.56$ – $2.64$  Å and two Ti(2A)–S(5) bonds that range from 2.74 to 2.81 Å. The long Ti(2A)–S(6) composite distance of  $\sim 3.3$  Å most likely represents a nonbonding interaction (i.e. square pyramid).

The M(3) sites contain solid solutions of lanthanum and titanium statistically disordered over two positions. The two metal sites lie approximately 1 Å from each other across a mirror plane at the center of a  $\text{S}_6$  octahedron formed by four S(3) atoms and two S(4) atoms (Figure 4). The lanthanum and titanium on the M(3) sites were constrained to give a total occupancy of 50%, which results in one metal atom per octahedron. The refined ratios of La:Ti are 0.140:0.360 in **I** and 0.062:0.438 in **II**. Once again, the metal and sulfur positions are composites of four different polyhedra; thus, the M–S distances are not accurate. However, on the basis of the general atom positions, one can conclude that lanthanum resides in a distorted octahedral environment, whereas titanium is best characterized as a distorted tetrahedron.<sup>2</sup> The M(3)–S(3) distances of  $\sim 3.2$  Å are too long to be considered Ti–S bonds but are reasonable La–S bonding distances.<sup>23</sup> The thermal ellipsoids at the M(3) site are suggestive of relatively invariant sulfur positions (isotropic shape) while the metal atom thermal ellipsoids are suggestive of displacement.

The M(3) site in **III** is essentially vacant with only a 6.4% titanium occupancy. It is similar to **I** and **II** in

that the metal atoms are disordered over the same two positions 1.3(2) Å apart from each other.

The tricapped trigonal prismatic La(1) $\text{OS}_8$  site that resides at the interstices of the two connecting layers has La(1)–O distances of 2.512(6), 2.509(6), and 2.546(7) Å for **I**, **II**, and **III**, respectively. The La(1)–S distances range from 2.840(3) to 3.113(1), 2.848(3) to 3.116(1), and 2.844(3) to 3.097(1) Å.

## Discussion

$\text{La}_{8.75}\text{Ti}_{9.25}\text{S}_{24}\text{O}_4$ ,  $\text{La}_{8.50}\text{Ti}_{9.50}\text{S}_{24}\text{O}_4$  and  $\text{La}_{8.10}\text{Ti}_{8.05}\text{S}_{24}\text{O}_4$  belong to a series of compounds described by the general formula  $\text{La}_{8+x}\text{Ti}_{8+y}\text{S}_{24}\text{O}_4$ , where  $(x + y) \leq 2$ . These oxysulfides possess an unusual combination of solid solution formation, vacancies, and site disorders that allow for changes in structure, composition, and titanium oxidation state. The stability of the  ${}^2_{\infty}[(\text{Ti}_4\text{S}_2\text{O}_4)(\text{TiS}_6)_{4/2}]^{(12+\delta)-}$  layer appears to force the adjoining sulfide layer to assemble regardless of composition. Aside from the previously reported compounds,  $\text{Sr}_{5.8}\text{La}_{4.4}\text{Ti}_{7.8}\text{S}_{24}\text{O}_4$  and  $\text{La}_{14}\text{Ti}_8\text{S}_{33}\text{O}_4$ , we have identified several other phases such as  $\text{La}_{23}\text{Ti}_{16.2}\text{S}_{57}\text{O}_8$  and  $\text{Bi}_{0.23}\text{La}_{13.77}\text{Ti}_8\text{S}_{33}\text{O}_4$  that have identical  ${}^2_{\infty}[(\text{Ti}_4\text{S}_2\text{O}_4)(\text{TiS}_6)_{4/2}]^{(12+\delta)-}$  layers. Despite the similarities in the oxysulfide layers, the interlayer compositions, interlayer structures, and overall compositions of the interleaving sulfide layers are very different. Thus the  ${}^2_{\infty}[(\text{Ti}_4\text{S}_2\text{O}_4)(\text{TiS}_6)_{4/2}]^{(12+\delta)-}$  framework serves as a host for a variety of guest metal sulfide intercalants but requires the intercalants to conform to the structural and spatial requirements generated by the oxysulfide layer.

In the  $\text{La}_{8+x}\text{Ti}_{8+y}\text{S}_{24}\text{O}_4$  series, the amount of flux and reaction conditions affect the product identity more than the compositions of the precursors. Unfortunately, we are unable to predict how these variables affect the product composition at this time. In contrast, the reaction temperature does seem to have a clear effect on the type of compound formed. Of all the lanthanum and titanium oxysulfides prepared to date,<sup>3,4,12</sup> heating temperatures of 1025–1050 °C are conducive to forming compounds with higher relative crystal symmetry, such as  $\text{La}_{8.75}\text{Ti}_{9.25}\text{S}_{24}\text{O}_4$ ,  $\text{La}_{8.50}\text{Ti}_{9.50}\text{S}_{24}\text{O}_4$ ,  $\text{La}_{8.10}\text{Ti}_{8.05}\text{S}_{24}\text{O}_4$ ,  $\text{Sr}_{5.8}\text{La}_{4.4}\text{Ti}_{7.8}\text{S}_{24}\text{O}_4$  (all tetragonal,  $P4/mmm$ ), and  $\text{La}_{20}\text{Ti}_{11}\text{S}_{44}\text{O}_6$  ( $Pmmm$ ). Lower temperature preparations give compounds such as  $\text{La}_{14}\text{Ti}_8\text{S}_{33}\text{O}_4$ <sup>4</sup> and  $\text{La}_{23}\text{Ti}_{16.2}\text{S}_{57}\text{O}_8$ ,<sup>12</sup> which have lower symmetry monoclinic cells ( $C2/m$ ). In the latter compounds, the symmetries of the oxysulfide layers are not crystallographically imposed, even though the layers are essentially identical. In other sulfide and oxysulfide compounds, we have found that large amounts of chloride can be incorporated into the structures when chloride fluxes are used in the synthesis.<sup>24</sup> In the present samples, however, EDX analysis on acid-washed crystals showed no detectable chloride signal in any of the compounds studied. Moreover, Cario et al. prepared  $\text{La}_8\text{Ti}_{10}\text{S}_{24}\text{O}_4$  without a chloride flux and obtained similar results.<sup>13</sup>

The disorder at the M(2) and M(3) sites is complicated and merits some discussion. All three compounds show the same type of disorder at M(2), with lanthanum and

(23) Using a bond valence method, the average La–S distance for a six-coordinate lanthanum is 2.90 Å.

(24) Litteer, J. B.; Fettingner, J. F.; Eichhorn, B. W. To be published.

titanium completely segregated to the center of a  $S_6$  octahedron and to the 4-fold disordered sites around the central atom, respectively. Because octahedral  $LaS_6$  moieties are not commonly observed, we performed neutron activation analysis (for La and Ti) in order to confirm our compositional assignments. Despite the differences in the Ti analysis, the La contents are in good agreement with the crystallographically refined compositions. The activation analysis, refined compositions, M–S distances, and variations in the unit cell parameters are all indicative of variable lanthanum occupation in the octahedral sites in this series of compounds. Lanthanum–titanium solid solution formation is also found in  $La_{23}Ti_{16.2}S_{57}O_8$ , which has monoclinic  $C2/m$  symmetry.<sup>12</sup> The M(2) site in this compound displays the same 4-fold symmetry; however, it is generated by two independent crystallographic positions that each contain a 2-fold disorder across a mirror plane (i.e. the 4-fold symmetry is not crystallographically imposed). The presence of the 4-fold disorder in this phase indicates that it is not an artifact of the high crystal symmetry of  $La_{8+x}Ti_{8+y}S_{24}O_4$  compounds. The  $La_{23}Ti_{16.2}S_{57}O_8$  phase also possesses the 2-fold disorder at the M(3) site, which is again not mandated by the lower symmetry monoclinic cell. It is interesting to note that the M(2) and M(3) sites of  $Sr_{5.8}La_{4.4}Ti_{7.8}S_{24}O_4$  were fully occupied but the 4-fold and 2-fold disorders were not present.<sup>4</sup>  $La_8Ti_{10}S_{24}O_4$  exhibits the same 2-fold disorder on the M(3) site as found in the  $La_{8+x}Ti_{8+y}S_{24}O_4$  compounds but is fully occupied by titanium. However, the Ti(2) site of  $La_8Ti_{10}S_{24}O_4$  did not exhibit a 4-fold disorder or any La occupation.<sup>13</sup>

The disordered metal sites in the  $La_{8+x}Ti_{8+y}S_{24}O_4$  series have two different effects on their host octahedra. At the M(2) $S_6$  site, which can be viewed as a composite of four  $TiS_5$  square pyramids and one  $LaS_6$  octahedron, there is a significant displacement of the four S(6) composite atoms in the  $a$ – $b$  plane (Figure 3). At the M(3) $S_6$  site, which can be viewed as a composite of two  $TiS_4$  tetrahedra and two  $LaS_6$  octahedra (for **II** and **III**), the sulfide ions appear fairly isotropic, whereas the metal atom sites show the effects of the composite

positions of La and Ti (Figure 4). The latter behavior is similar to that observed in  $La_4Ti_3S_4O_8$ .<sup>2</sup>

Assuming that the charges on La, S, and O are +3, –2, and –2, the average oxidation state of titanium is +3.22, +3.21, and +3.94 for  $La_{8.75}Ti_{9.25}S_{24}O_4$ ,  $La_{8.50}Ti_{9.50}S_{24}O_4$ , and  $La_{8.10}Ti_{8.05}S_{24}O_4$ , respectively. Compound **III** contains essentially all  $Ti^{4+}$ ; however, assigning the oxidation states of titanium in **I** and **II** is difficult due to the complicated disorder, composite atom positions, and our inability to distinguish  $Ti^{3+}$  centers from bond valence calculations.<sup>15,16</sup> We do know that for **I** and **II**, there are only two  $Ti^{4+}$  atoms per formula unit. As a result, both the oxysulfide and the disordered sulfide layer must contain reduced titanium. It is possible that the charge on the titanium atoms is delocalized throughout the structure. Compound **III** has a shorter Ti(5)–O(1) distances at 1.937(7) Å compared to 1.960(6) and 1.958(6) Å for **I** and **II**, respectively. This may be an indication of a reduced Ti(5) center for **I** and **II**, as one would expect longer Ti–O distances for  $Ti^{3+}$  centers versus  $Ti^{4+}$  centers (VI coordinate  $Ti^{3+}$ ,  $r_i = 0.67$  Å; VI coordinate  $Ti^{4+}$ ,  $r_i = 0.605$  Å).<sup>22</sup> The presence of reduced titanium in the  $Ti_4S_2O_4$  cluster is in agreement with the proposal of Deudon et al. that the  $Ti_4S_2O_4$  clusters in  $La_{20}Ti_{11}S_{44}O_6$  contain  $Ti^{3+}$  centers.<sup>3</sup> The  ${}_{\infty}[(Ti_4S_2O_4)(TiS_6)_{4/2}]^{(12+\delta)-}$  oxysulfide layer can contain either all  $Ti^{4+}$  centers, as shown in **III**, or predominately  $Ti^{3+}$  centers, as evidenced in **I** and **II**, without major structural variations.

**Acknowledgment.** We gratefully acknowledge the NSF-DMR (#9223060) and the Electric Power Research Institute for support. The authors wish to acknowledge the Nuclear Methods Group at the National Institute of Standards and Technology for the use of the shared equipment at the INAA high rate counting facility.

**Supporting Information Available:** Complete listing of crystallographic data for I–III (56 pages); observed and calculated structure factors (6 pages). See any current masthead page for ordering information.

CM970663O